Journal of Sound and Vibration (2000) **231**(4), 1039–1055
doi:10.1006/jsvi.1999.2627, available online at http://www.idealibrary.com on IDEAL®

DYNAMIC RESPONSE OF ADAPTIVE CANTILEVERS CARRYING EXTERNAL STORES AND SUBJECTED TO BLAST LOADING

SUNGSOO NA

Department of Automation Engineering, Korea Polytechnic University, Shihung City, Kyonggi-Do, 429-450, *Korea*

AND

LIVIU LIBRESCU

Department of Engineering Science and Mechanics, Virginia Polytechnic Institute and State University, Blacksburg, VA 24061, *U.S.A.*

(*Received* 1 *March* 1999, *and in final form* 29 *July* 1999)

This paper deals with the control of the dynamic response of cantilevered thin-walled beams carrying externally mounted stores and exposed to time-dependent external excitations. In this context, and toward this goal, the adaptive materials technology is used. A feedback control law relating the piezoelectrically induced bending moment at the beam tip with the angular velocity at the same point of the structure is considered, and its effects on the closed-loop dynamic response is investigated. The obtained results reveal that this control methodology can play a noticeable role toward confining the oscillations of the considered structure when exposed to blast loadings.

1. INTRODUCTION

The dynamic response of elastic structures under time-dependent external excitations is a subject of much interest in the design of aeronautical and aerospace vehicles. Such time-dependent external excitations may be induced by atmospheric turbulence, nuclear blast, sonic boom, shock wave, fuel explosion, etc.

Due to the damaging effects upon the structural integrity and operational life of these vehicles, adequate methods to predict and control their structural dynamic response have to be devised. This is imperative, as the next generations of aeronautical and space vehicles are likely to feature increasing structural flexibility and operate in severe environmental conditions.

Civil and military airplane wings are designed to carry heavy external mounted stores along their span. Depending on their magnitude and location, drastic reduction of natural eigenfrequencies and modification of the eigenmodes are experienced [1–3]. These modifications can result in a deterioration of the dynamic

0022-460X/00/141039 + 17 $35.00/0

response to time-dependent excitations and can also precipitate the occurrence of the flutter instability [4–6].

One of the possible options enabling one to control the dynamic response of these structures under time-dependent external excitations and eliminate their damaging effects without weight penalties, consists of the incorporation of adaptive materials technology.

In a structure featuring adaptive capabilities, the dynamic response characteristics can be controlled in a known and predictable manner and, as a result, one can avoid the occurrence of the structural resonance and of any dynamic instability and enhance the dynamic response to transient loadings [7, 8].

The adaptive capability can be achieved through the converse piezoelectric effect, which consists of the generation of localized strains in response to an applied voltage. This induced strain field produces, in turn, a change in the dynamic response characteristics of the structure. Employment of a control law relating the applied electric field with one of the kinematical response quantities according to a prescribed functional relationship, results in a dynamic boundary-value problem whose solution yields the closed-loop dynamic response characteristics.

Based upon the adaptive materials control technology, in the forthcoming developments, the control of the dynamic response of cantilevered structures carrying externally mounted stores and exposed to time-dependent excitations will be addressed.

In addition to airplane wings, robot manipulator arms operating in space, space booms and space telescopes are also cantilevered-type structures. These are required to be lightweight, strong and capable of high precision under the action of heavy masses located along their span. As a result, the control methodology considered in this paper extends also to such structures.

2. GENERAL CONSIDERATIONS, BASIC ASSUMPTIONS

The case of cantilevered thin-walled beams of arbitrary closed cross-section is considered. It is assumed that the beam is symmetrically composed of transversely isotropic material layers, the surface of isotropy in each material layer being parallel to the reference surface of the beam structure.

It is further assumed that the beam carries along its span a system of concentrated stores of mass m_j and mass moment of inertia I_{oj} (about their centroid) located at $z = z_j$, $(j = \overline{1, \ldots, J})$, where J denotes the total number of wing-mounted stores (see Figure 1). It is also postulated that within present analysis the case of tip-stores is not included.

Two systems of co-ordinates are used in the forthcoming developments, namely: (1) a *global* Cartesian system (x, y, z) where (x, y) denote the cross-section beam co-ordinates while the spanwise z-axis is assumed to coincide with the locus of symmetrical points of the cross-sections along the wing span, and (2) a *local* orthogonal co-ordinate system (n, s, z) where n denotes the thicknesswise co-ordinate normal to the beam mid-surface and s the tangential co-ordinate along the contour line of the beam cross-section (see Figure 1).

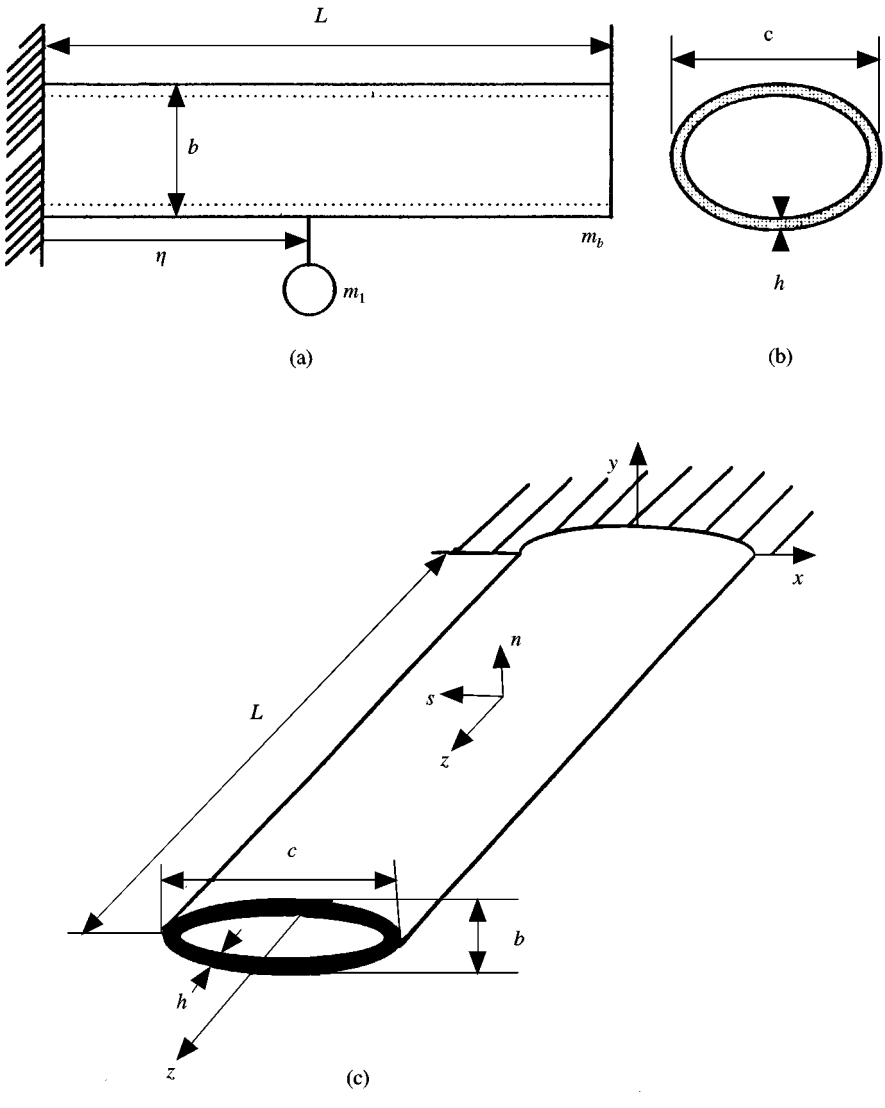

Figure 1. Geometry of the cantilever beam carrying one store—three views of it: (a) lateral view, (b) front view, (c) top view.

The equations governing the motion of cantilever beams are established in the context of the following assumptions: (1) the cross-sections of the beam do not deform in their own planes, (2) the effects of transverse shear flexibility featured by the advanced composite materials are taken into consideration, (3) the hoop stress resultant N_{ss} is considered negligible with respect to the remaining ones, and (4) the centroids of the attached masses are distributed along the z-axis.

As a result of transverse isotropy of the constituent materials and of assumption (4), an exact decoupling of transverse bending (expressed in terms of variables v_0 and θ_x), lateral (i.e., chordwise) bending (expressed in terms of u_0 and θ_y) and twist (Θ) is obtained. For the problem studied herein only the transverse bending

will be considered. However, since secondary warping induces transverse bending [9], this effect will also be incorporated.

We assume that the master structure consists of m layers, and that the actuators consisting of l piezoelectric layers are distributed over the entire span of the beam. As shown in references, [11–15], piezoactuators featuring transverse isotropic properties (with the plane of isotropy parallel to the mid-surface of the beam), spread over the entire beam span and bonded symmetrically on the outer and inner faces of the beam, but activated out-of-phase, generate a bending moment at the beam tip in response to a thicknesswise electric field $\mathscr{E}_3$.

3. GOVERNING SYSTEM

Based upon the previously stipulated assumptions, for a thin-walled beam carrying stores along its span the equations governing the flexural motion about the equilibrium position, as derived in references [1–3] are

$$a_{55}(v_0'' + \theta_x') - \left[b_1 \ddot{v}_0 + \sum_{j=1}^{J} m_j \ddot{v}_0 \delta(z - z_j) \right] + p_y = 0, \tag{1a, b}$$

$$a_{33}\theta_x'' - a_{55}(v_0' + \theta_x) - \left[(b_4 + b_{14})\ddot{\theta}_x + \sum_{j=1}^{J} I_j \ddot{\theta}_x \delta(z - z_j) \right] = 0,$$

where $z_j < L$, L being the span of the beam. Herein and in the remaindor, the terms identified by a dotted line are associated with rotatory inertia effect.

For the beam considered to be clamped at the root and free at the tip, the associated boundary conditions are

$$v_0 = \theta_x = 0 \quad \text{at } z = 0 \tag{2a, b}$$

and

$$\begin{aligned} &a_{55}(v_0' + \theta_x) = 0, \\ &a_{33}\theta_x' = \hat{M}_x. \end{aligned} \quad \text{at } z = L. \tag{3a, b}$$

Herein $v_0(z, t)$ and $\theta_x(z, t)$ denote the transverse deflection and rotation about the x-axis, respectively, $\delta(\cdot)$ denotes the Dirac's distribution, and a_{33} and a_{55} denote the bending and transverse shear stiffness, respectively. These are defined as

$$a_{33} = \oint_C \left[\bar{K}_{11} y^2 + \bar{\bar{K}}_{11} \left(\frac{dx}{ds} \right)^2 \right] ds, \qquad a_{55} = \oint_C \left[A_{66} \left(\frac{dy}{ds} \right)^2 + A_{44} \left(\frac{dx}{ds} \right)^2 \right] ds, \tag{4a, b}$$

where

$$\bar{K}_{11} = A_{11} - A_{12}^2/A_{11}, \qquad \bar{\bar{K}}_{11} = D_{11}, \tag{5a, b}$$

while

$$(A_{ij}, D_{ij}) = \sum_{k=1}^{N} \int_{n_{(k-1)}}^{n_{(k)}} \tilde{C}_{ij}^{(k)}(1, n^2)\, dn \tag{6}$$

denote the stretching and bending stiffness quantities, respectively, and N denotes the number of constituent layers.

In equations (6), $\tilde{C}_{ij}$ denote the reduced elastic coefficients, that, for the present type of anisotropy, are expressed in terms of the engineering constants as

$$\tilde{C}_{11} = \tilde{C}_{22} = \frac{E}{1 - v^2}, \qquad \tilde{C}_{12} = \frac{Ev}{1 - v^2}, \tag{7a–d}$$

$$\tilde{C}_{66} = G(\equiv E/2(1 + v)), \qquad \tilde{C}_{44} = \tilde{C}_{55} = G'.$$

In these expressions, E and v denote Young's modulus and Poisson's ratio in the plane of isotropy, respectively, while G' and G denote the transverse shear and the in-plane shear modulus, respectively.

In addition,

$$(b_1, b_4) = \oint_C m_0(1, y^2)\,\mathrm{d}s, \qquad b_{14} = \oint_C m_2 \left[\frac{\mathrm{d}x}{\mathrm{d}s}\right]^2 \mathrm{d}s \tag{8a, b}$$

stand for the mass terms, where

$$(m_0, m_2) = \sum_{k=1}^{N} \int_{h_{(k-1)}}^{h_{(k)}} \rho_{(k)}(1, n^2)\,\mathrm{d}n, \tag{9}$$

ρ denotes the mass density of the constituent materials, and p_y ($\equiv p_y(z, t)$) is the distributed lateral load per unit span of the beam.

The primes denote derivatives with respect to the spanwise z-co-ordinate while the superposed dots denote derivatives with respect to time t, $\oint_C(\cdot)\,\mathrm{d}s$ denotes the integral around the circumference of the mid-line contour of the beam.

In the boundary condition (36), $\hat{M}_x$ denotes the piezoelectrically induced bending moment which, for already mentioned reasons (see references [7, 8, 10, 11, 13–15]), appears only in the boundary conditions at $z = L$.

4. SPECIAL CASE OF GOVERNING EQUATIONS

The Bernoulli–Euler counterpart of the governing equations (1) and boundary conditions, equations (2) and (3) are obtained through the elimination of $a_{55}(v_0' + \theta_x')$ in equations (1) and (3), this operation followed by consideration of $\theta_x = -v_0'$. In such a way, the equation governing the transverse bending of thin-walled beams carrying concentrated masses are reduced to

$$a_{33} v_0'''' - \left[(b_4 + b_{14})\ddot{v}_0'' + \sum_{j=1}^{J} I_j \ddot{v}_0'' \delta(z - z_j)\right] + \left[b_1 \ddot{v}_0 + \sum_{j=1}^{J} m_j \ddot{v}_0 \delta(z - z_j)\right] = p_y, \tag{10}$$

while the boundary conditions to be prescribed are

$$v_0 = v_0' = 0 \quad \text{at } z = 0 \tag{11a, b}$$

and

$$\begin{matrix} a_{33}v_0''' = 0 \\ a_{33}v_0'' = \hat{M}_x \end{matrix} \quad \text{at } z = L, \tag{12a, b}$$

It should be remarked that both the shearable and the classical non-shearable thin-walled beam models provide fourth order governing equation systems.

5. TIME-DEPENDENT LOADS ASSOCIATED WITH BLAST AND SONIC BOOM

Various time-dependent loads will be considered in the analysis of the dynamic response. Among these, explosive blast and sonic-boom pulses will be included.

For the case of blast loadings, various analytical expressions have been proposed and discussed [17, 18]. As it was clearly established, the blast wave reaches the peak value in such a short time that the structure can be assumed to be loaded instantly. Based on the experimental evidence, it may also be assumed that the pressure is uniformly distributed over the beam. This fact is also assumed in the case of sonic-boom pulses. In accordance with the above-mentioned references, the overpressure associated with the blast pulses can be described in terms of the modified Friedlander exponential decay equation as

$$p_y(s, z, t)(\equiv p_y(t)) = P_m\left(1 - \frac{t}{t_p}\right)\mathrm{e}^{-a't/t_p}, \tag{13}$$

where the negative phase of the blast is included. In equation (13), P_m denotes the peak reflected pressure in excess of the ambient one, t_p denotes the positive phase duration of the pulse measured from the time of impact of the structure and a' denotes a decay parameter which has to be adjusted to approximate the overpressure signature from the blast tests. As it could be inferred, the triangular blast load may be viewed as a limiting case of equation (13), occurring when $a'/t_p \to 0$.

As concerns the sonic-boom loading, this can be modelled as an N-shaped pressure pulse arriving at a normal incidence. Such a pulse corresponds to an idealized farfield overpressure produced by an aircraft flying supersonically in the earth's atmosphere or by any supersonic projectile rocket or missile [18–21]. The overpressure signature of the sonic-boom shock pulse can be described by

$$p_y(s, z, t)(\equiv p_y(t)) = \begin{cases} P_m\left(1 - \dfrac{t}{t_p}\right) & 0 < t < rt_p, \\ 0 & \text{for } t < 0 \text{ and } t > rt_p, \end{cases} \tag{14}$$

where r denotes the shock pulse length factor, and P_m and t_p maintain the same meaning as in the case of blast pulses. It may readily be seen that (1) for $r = 1$ the sonic-boom pulse degenerates into a triangular pulse; (2) for $r = 2$ a symmetric sonic-boom pressure pulse is obtained; while (3) for $1 < r < 2$ the pressure pulse becomes an asymmetric one. The dynamic response of composite flat panels to such shock pulses was analyzed in references [20, 21].

Another special case corresponds to a step pulse. Its analytic description can be either obtained from equation (13), when $t_p \to \infty$, or from equation (14) when $r = 1$ and $t_p \to \infty$.

In addition, the case of the rectangular pressure pulse is also considered and described as

$$p_y(s, z, t) \equiv p_y(t) = \begin{cases} P_m, & 0 \leqslant t \leqslant t_p, \\ 0, & t > t_p. \end{cases} \tag{15}$$

6. THE CONTROL LAW, CLOSED-LOOP SOLUTION METHODOLOGY

One of the possible ways towards controlling the dynamic response of cantilevered beams carrying external stores is via the generation and use of a dynamic bending moment acting at the beam tip, method referred to as the *boundary moment control.*

Such a bending moment control can be generated by incorporating piezoactuators into the structure and using the converse effect featured by these devices. Structures with embedded or bonded piezoactuators belong to the class of *intelligent structures.* A comprehensive review and assessment of the state of the art in the use of intelligent structures for aerospace applications can be found in reference [22].

As shown [3, 7, 8, 11], piezoactuators featuring in-plane isotropic properties, spread over the entire span of the beam and bonded symmetrically on the outer and inner faces of the beam, but activated out of phase, generate a bending moment at the beam tip in response to an electric field $\mathscr{E}_3$.

For feedback control, the applied electric field $\mathscr{E}_3$ upon which the piezoelectrically induced moment depends, should be expressed, through a prescribed functional relationship with one of the mechanical quantities characterizing the beam's response. In this regard, a number of control laws can be implemented. For the problem at hand, the goal of the control is to enhance the free vibration behavior, inhibit the forced vibration response to time-dependent external excitations and prevent resonance.

In contrast to previously used feedback control laws [1–3, 7, 11], that have merely a static character, and in agreement with the control methodologies used in references [8, 10, 14, 16], *velocity feedback control* appears to be highly indicated for the problem at hand. According to this control law [7, 8], $\hat{M}_x$ is proportional to the rotational velocity $\dot{\theta}_x(L, t)$ at the wing tip, implying $\hat{M}_x(L, t) = -k_v \dot{\theta}_x(L, t)$ so that boundary conditions (3b) can be cast as

$$\theta'_x(L, t) = (k_v/a_{33})\dot{\theta}_x(L, t), \tag{16}$$

where k_v is the feedback gain. The advantage of this dynamic control law consists, among others, in the possibility to generate damping. The methodology used to solve the present dynamic response problems is shortly described next.

The solution of the dynamic response problem is based on the extended Galerkin method. To this end, Hamilton's variational principle is used, by virtue of which

$$\int_{t_1}^{t_2} (\delta T - \delta V + \delta W)\, \mathrm{d}t = 0, \qquad \delta v_0 = \delta \theta_x = 0 \quad \text{at } t = t_1, t_2. \tag{17}$$

Here T and V denote the kinetic and strain energies, respectively, while W is the work done by the external distributed loads and body forces; t_1 and t_2 denote two arbitrary instants of the time t, while δ denotes the variational operator.

For the problem at hand V and T assume the form

$$V = \frac{1}{2}\int_0^L [a_{33}(\theta_x')^2 + a_{55}(\theta_x + v_0')^2]\,\mathrm{d}z,$$

$$T = \int_0^L [b_1 \dot{v}_0^2 + (b_4 + b_{14})\dot{\theta}_x^2]\,\mathrm{d}z + \sum_{j=1}^{J} m_j \dot{v}_0^2(z_j) + \sum_{j=1}^{J} I_j \dot{\theta}_x^2(z_j), \tag{18a, b}$$

whereas the virtual work due to the boundary moment $\hat{M}_x$ and the load p_y is given by

$$\delta W = \hat{M}_x \delta\theta_x(L, t) + p_y(z, t)\delta v_0(z, t). \tag{18c}$$

Considering equation's (18) in equation (17), and performing the indicated operations can result in equation's (1)–(3). However, in order to discretize the boundary value problem, we will represent $v_0(z, t)$ and $\theta_x(z, t)$ by means of series of space-dependent trial functions which have to fulfill all the kinematic boundary conditions multiplied by time-dependent generalized co-ordinates whose determination constitutes the central goal of the dynamic response. These representations are

$$v_0(z, t) = \mathbf{V}^{\mathrm{T}}(z)\mathbf{q}_v(t), \qquad \theta_x(z, t) = \mathbf{W}^{\mathrm{T}}(z)\mathbf{q}_w(t), \tag{19a, b}$$

where

$$\mathbf{V} = [V_1\ V_2\ \ldots\ V_N]^{\mathrm{T}}, \qquad \mathbf{W} = [W_1\ W_2\ \ldots\ W_N]^{\mathrm{T}}, \tag{20a, b}$$

are the vectors of trial functions, while

$$\mathbf{q}_v = [q_1^v\ q_2^v\ \ldots\ q_N^v], \qquad \mathbf{q}_w = [q_1^w\ q_2^w\ \ldots\ q_N^w], \tag{21a, b}$$

are the vectors of generalized co-ordinates. Substitution of equations (19)–(21) and of representation of time-dependent loads into equation (18c), performing the required integration with respect to the spanwise z-co-ordinate and the time t, and enforcing Hamilton's conditions $\delta\mathbf{q} = 0$ at $t = t_1, t_2$, one obtains the discrete governing equations

$$\mathbf{M}\ddot{\mathbf{q}}(t) + \mathbf{H}\dot{\mathbf{q}}(t) + \mathbf{K}\mathbf{q}(t) = \mathbf{Q}(t). \tag{22}$$

In equation (22), $\mathbf{q}(t)$ is the $2N \times 1$ generalized co-ordinate column vector, $\mathbf{M}$, $\mathbf{H}$, and $\mathbf{K}$ are $2N \times 2N$ square matrices, corresponding to mass, damping and stiffness, respectively, while $\mathbf{Q}(t)$ is the $2N \times 1$ generalized input force vector. The boundary conditions at $z = L$ being in general not fulfilled, corrective terms instead of zero-valued ones appear in the process of integration of equation (17), terms which compensate the non-fulfillment of the non-essential boundary conditions. Such corrective boundary terms appear in the elements of the matrix $\mathbf{K}$. The expressions

of these matrices are

$$\mathbf{M} = \int_0^L \begin{bmatrix} b_1 \mathbf{V}\mathbf{V}^{\mathrm{T}} & 0 \\ \mathbf{0} & (b_4 + b_{14})\mathbf{W}\mathbf{W}^{\mathrm{T}} \end{bmatrix} \mathrm{d}z + \begin{bmatrix} \sum_{j=1}^{J} m_j(z_j)\mathbf{V}(z_j)\mathbf{V}^{\mathrm{T}}(z_j) & 0 \\ 0 & \sum_{j=1}^{J} I_j \mathbf{W}(z_j)\mathbf{W}^{\mathrm{T}}(z_j) \end{bmatrix},$$

$$\mathbf{H} = \begin{bmatrix} 0 & 0 \\ 0 & k_v \mathbf{W}(L)\mathbf{W}^{\mathrm{T}}(L) \end{bmatrix}, \quad K = \int_0^L \begin{bmatrix} a_{55}\mathbf{V}'\mathbf{V}'^{\mathrm{T}} & a_{55}\mathbf{V}'\mathbf{W}^{\mathrm{T}} \\ Symm & a_{55}\mathbf{W}\mathbf{W}^{\mathrm{T}} + a_{33}\mathbf{W}'\mathbf{W}'^{\mathrm{T}} \end{bmatrix} \mathrm{d}z,$$

$$\mathbf{Q} = \int_0^L p_y \mathbf{V}^{\mathrm{T}} \, \mathrm{d}z. \tag{23a–d}$$

It clearly appears from equation (23b) that in the absence of the structural damping (which is the case considered here), and of the unactivated beam (implying $k_v = 0$), the damping matrix $\mathbf{H}$ becomes immaterial.

A solution of equation (22) can be obtained by casting it in the state-space form (see reference [24]). To this end, we define the state vector $\mathbf{X} = [\mathbf{q}^{\mathrm{T}} \, \dot{\mathbf{q}}^{\mathrm{T}}]^{\mathrm{T}}$ and adjoin the identity $\dot{\mathbf{q}} \equiv \dot{\mathbf{q}}$. As a result, equation (22) modifies as

$$\dot{\mathbf{X}}(t) = \mathbf{A}\mathbf{X}(t) + \mathbf{B}\mathbf{Q}(t), \tag{24}$$

where

$$\mathbf{A} = \begin{bmatrix} 0 & I \\ -\mathbf{M}^{-1}\mathbf{K} & -\mathbf{M}^{-1}\mathbf{H} \end{bmatrix}, \quad \mathbf{B} = [\mathbf{0} \quad \mathbf{M}^{-1}]^{\mathrm{T}} \tag{25a, b}$$

are coefficient matrices.

For the free vibration problem, the homogeneous solution of equation (24) has the form $\mathbf{X}(t) = \mathbf{x}\mathrm{e}^{\lambda t}$ where $\mathbf{x}$ is a constant vector and λ is a constant scalar, both generally complex. With this, a standard eigenvalue problem is obtained,

$$\mathbf{A}\mathbf{x} = \lambda \mathbf{x} \tag{26}$$

that can be solved for the eigenvalues λ_r and eigenvectors $x_r (r = 1\mathrm{m}\,2, \ldots)$. The solution of the algebraic eigenvalue problem yields the closed-loop eigenvalues

$$(\lambda_r, \bar{\lambda}_r) = \sigma_r \pm \mathrm{i}\omega_{dr}, \tag{27}$$

where σ_r is a measure of the induced damping in the rth mode and ω_{dr} is the rth frequency of damped oscillation.

7. NUMERICAL ILLUSTRATIONS AND DISCUSSION

The numerical illustrations concern the open and closed-loop dynamic response of a cantilevered thin-walled beam of biconvex cross-section profile (see Figure 1) subjected to transient loadings. This cross-section profile was used

in the study of the aeroelastic behavior of advanced aircraft wings in references [7 and 8].

The host structure is considered to consist of a transverse isotropic material whose isotropy surface is parallel at each point to the mid-surface of the beam, and the piezoactuators are made-up from PZT-4 piezoceramic whose properties are displayed in [25] (see also reference [12]).

Throughout the numerical illustrations, unless otherwise stated, it was considered, that $E/G' = 50$; $L = 1$ m; $b = 0{\cdot}068$ m and $c = 0{\cdot}25$ m; $h_a = 0{\cdot}2 \times 10^{-3}$ m; $h = 0{\cdot}68 \times 10^{-1}$ m; $m_1/m_b = 0{\cdot}1$, where m_1 and m_b are the store and beam mass, respectively. The considered dimensions correspond to a beam of aspect ratio, $AR\ (\equiv 2L/c) = 8$ and the response quantities displayed in the plots are associated with the beam tip cross-section, $z = L$.

Moreover, the results have been generated for the case of zero initial conditions and of $P_m = 500lb/L$. In the following numerical illustrations, the non-dimensional feedback gain, related to its dimensional counterpart is defined as

$$K_v = k_v \bar{\omega} L / a_{33}, \tag{28}$$

where $\bar{\omega} = 128{\cdot}16$ rad/s is a open-loop reference natural frequency corresponding to a beam characterized by $E/G' = 50$ and $AR = 16$.

In Figure 2, there is highlighted the effect of the proposed control methodology on the dynamic response $\tilde{V} \equiv V_0/L$ of a shearable cantilevered beam whose constituent material features a transverse shear flexibility ratio measured in terms of the ratio $R(\equiv E/G') = 50$, carrying a store and subjected to a blast load (indicated in the inset of the figure).

The results show that within the forced motion regime (i.e., for $t < 0{\cdot}03$ s) the implemented control methodology is much less effective than within the free motion regime (i.e., for $t > 0{\cdot}03$ s). At the same time, the results reveal that for the case of the store located towards the beam tip, a less-efficient control is achieved as compared to that of the store located toward the middle of the beam, in the sense that the decay of the deflection amplitude is slower in the former instance than in the latter one.

The control of dynamic response to sonic-boom pressure waves is displayed in Figure 3. Herein the influence of transverse shear flexibility on dynamic response of a beam carrying an unistore located toward the beam tip ($\eta = 0{\cdot}9$) is addressed, where $\eta(\equiv z/L)$ denotes the dimensionless spanwise co-ordinate. In this sense, $E/G' = 0$ and $E/G' = 100$ correspond to Bernoulli–Euler and shear-deformable beams, respectively, where E/G' constitutes a measure of transverse shear flexibility the beam material. Within the next developments, these two cases are referred to as unshearable and shearable beams, respectively.

The results of this plot reveal that the unshearable beam model underestimates the deflection featured by the actual, shearable beam. However, for the activated beam in the free motion regime (i.e., when $t > rt_p = 0{\cdot}0375\ s$), the amount of difference between the closed-loop dynamic response amplitudes of shearable and unshearable beams appears to be very small. In addition, from this graph the efficiency of the implementation of this control methodology becomes fully evident.

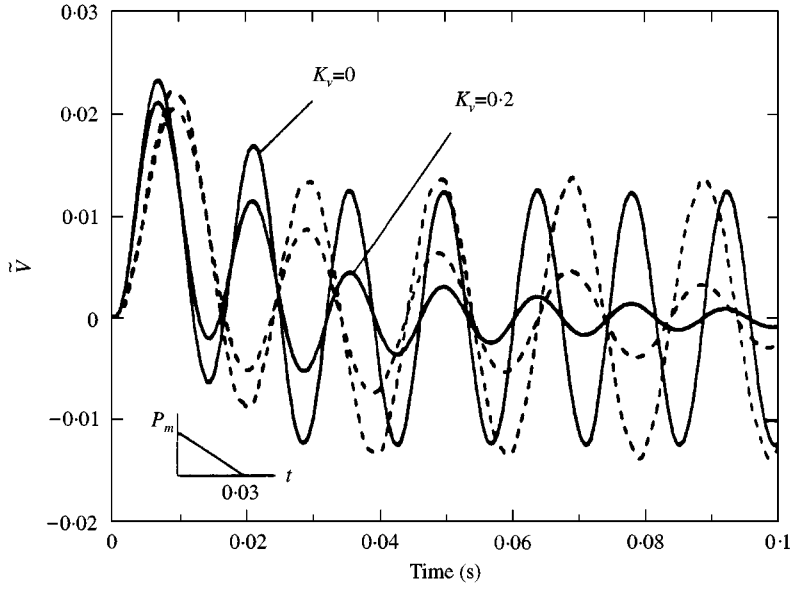

Figure 2. Dimensionless transverse deflection time-history of thin-walled beams to a triangular blast load for two locations of the unistore: ——, $\eta = 0{\cdot}5$; and - - - - -, $\eta = 0{\cdot}9$. The results for $K_v = 0$ and $K_v = 0{\cdot}2$ correspond to the open and closed-loop dynamic response respectively. The material of the host structure is characterized by $E/G' = 50$, while $m_1/m_b = 0{\cdot}5$.

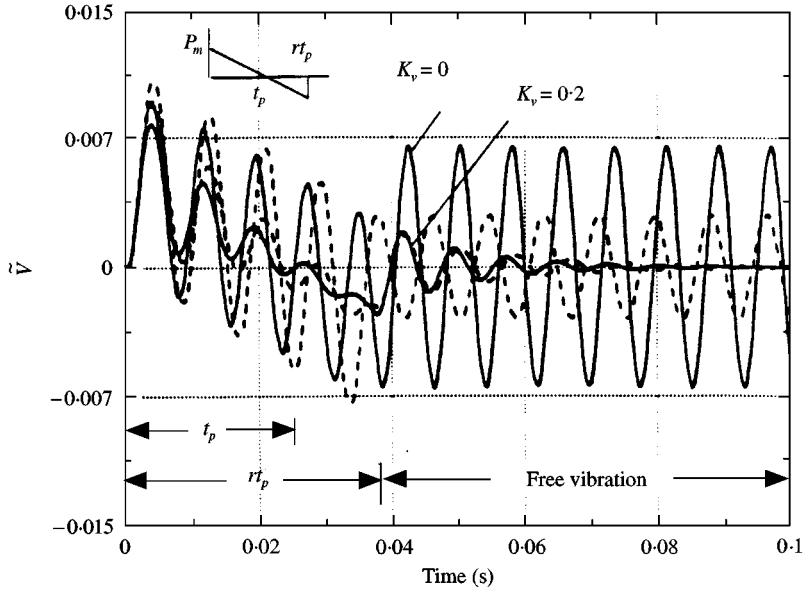

Figure 3. Dynamic response control of a thin-walled beam to a sonic-boom pressure pluse characterized by $r = 1{\cdot}5$; $t_p = 0{\cdot}025$ s. The beam is characterized by an aspect ratio $AR = 6$, and the unistore of $m_1/m_b = 0{\cdot}1$ is located at $\eta = 0{\cdot}9$. The material of the host structure is characterized by $E/G' = 0$ (——) and $E/G' = 100$ (- - - - -).

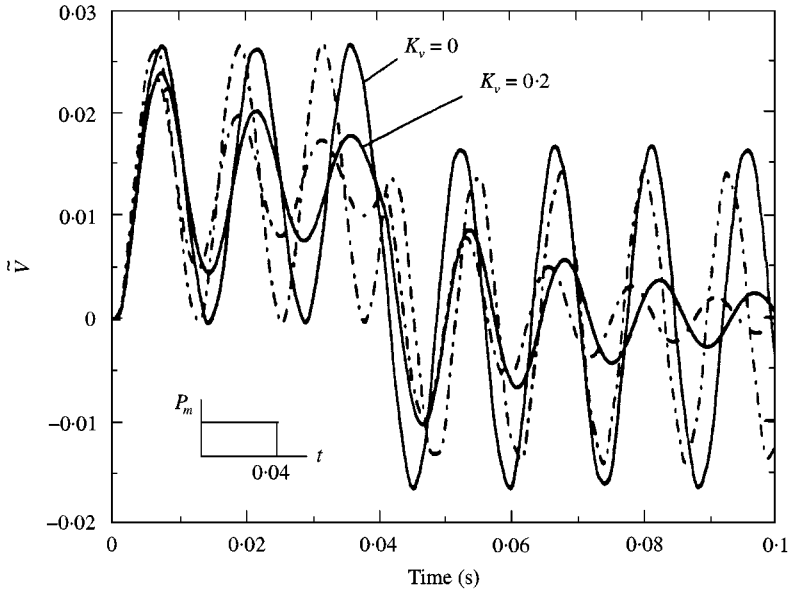

Figure 4. Dynamic response to a rectangular pulse of a shearable thin-walled beam carrying a unistore exposed to Open ($K_v = 0$) and closed-loop ($K_v = 0{\cdot}2$) responses. Two locations of the unistore are considered, namely $\eta = 0{\cdot}1$ (—·—·) and $\eta = 0{\cdot}9$ (——).

One should also remark that, within the velocity feedback control, the closed-loop eigenvalues are complex valued quantities, and as a result, damping is generated [8, 10, 11]. This explains why for the activated structure, and in contrast to the non-activated one, the response amplitude decays as time unfolds.

In Figure 4 the control of a cantilevered beam carrying one store and exposed to a rectangular pressure pulse is considered. The results reveal that a more efficient control is achieved when the store is located toward the beam root than toward its tip, (i.e., when $\eta = 0{\cdot}1$), a conclusion which is specially true in the free-motion regime.

In conjunction with the effect of transverse shear flexibility on the dynamic response of cantilevered beam to a rectangular pulse, the results emerging from Figure 5 reveal a trend similar to that in Figure 3, in the sense that the discard of transverse shear effect results in an underestimation of the deflection amplitude as compared to the actual one, featured by the shearable beam model. However, this underestimation is less accentuated for the activated beam than for the non-activated one.

The effect of transverse shear flexibility of the material of the host structure on the open and closed-loop deflection time history is displayed also in Figure 6, where the beam carrying a store is exposed to a step pulse. In addition to the efficiency of this control methodology, the results reveal again that the classical beam model underestimates the deflection amplitude of both the closed and open-loop dynamic responses. Having in view that, due to the piezoelectrically induced damping, the closed-loop dynamic response amplitude decays as time unfolds, the classical beam model discarding transverse shear effect, underestimates the time at which the structure is brought to rest.

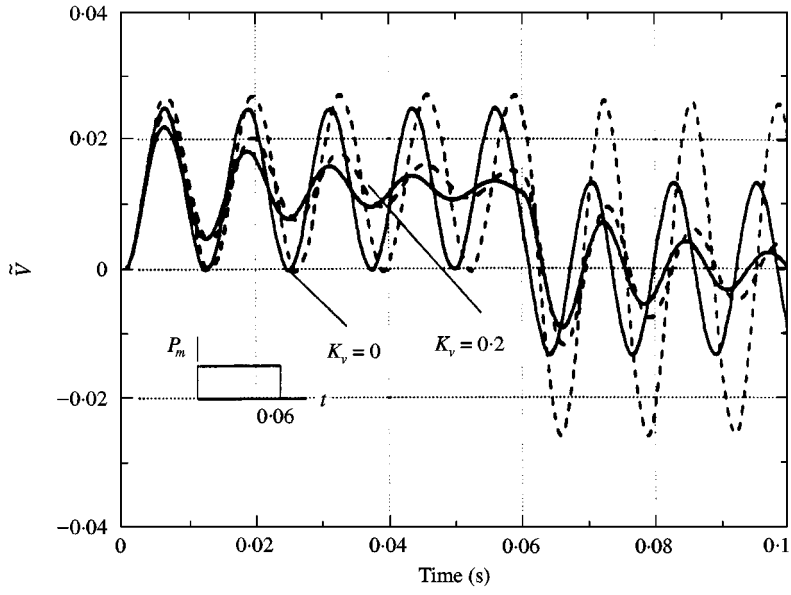

Figure 5. Dynamic response of shearable, $E/G' = 100$, (- - - - -) and unshearable $E/G' = 0$, (——), thin-walled beams to a rectangular pressure-pulse. Unistore of $m_1/m_b = 0{\cdot}1$ at $\eta = 0{\cdot}5$.

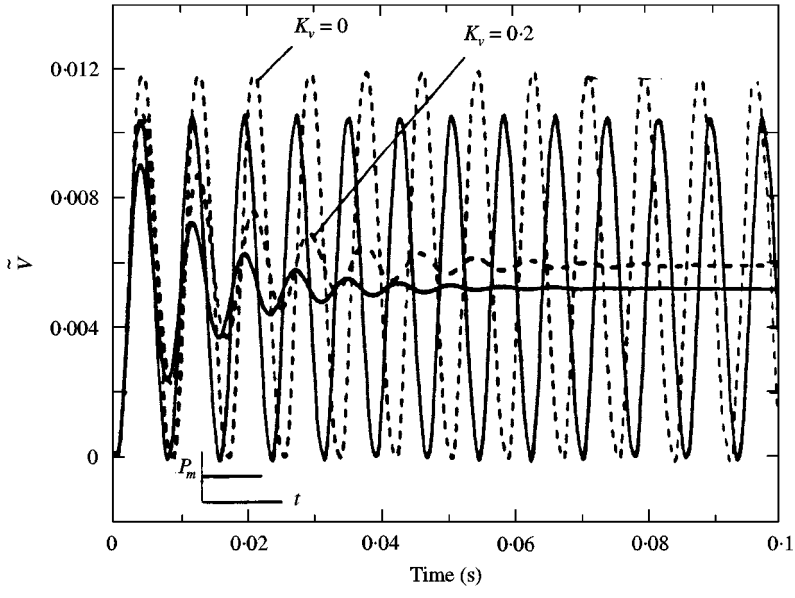

Figure 6. Dynamic response of a thin-walled beam carrying an unistore ($m_1/m_b = 0{\cdot}1$; $\eta = 0{\cdot}9$), exposed to a step pulse. Classical $E/G' = 0$, (——), and shearable, $E/G' = 100$, (- - - - -) beam models.

In Figure 7, the dynamic response of the clean beam and of that carrying a store located towards the beam tip, ($\eta = 0{\cdot}9$), subjected to a step pressure pulse is presented. As is evident from this figure, the oscillations tend to decay faster for the clean beam than for the beam counterpart carrying a store.

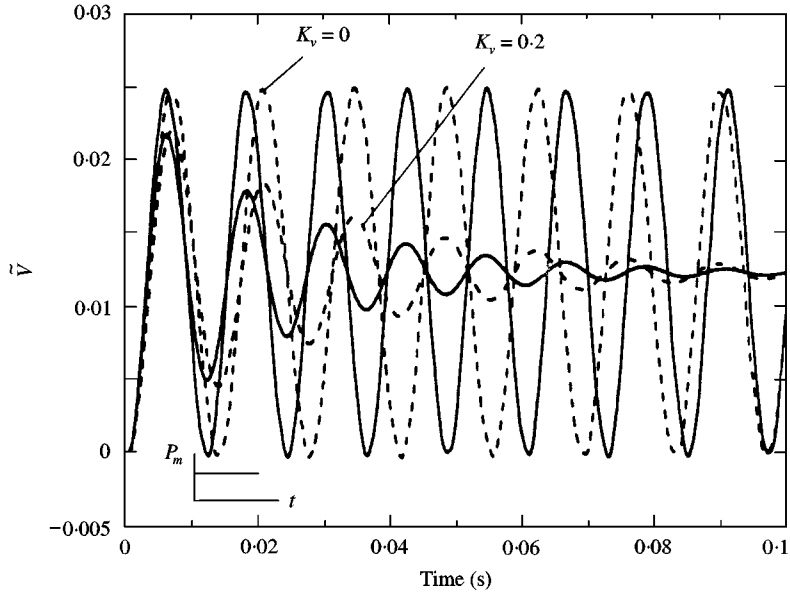

Figure 7. Comparisons of the dynamic response to a step pulse of a thin-walled unshearable beam ($E/G' = 0$), in the cases of no store (——), and unistore located at $\eta = 0{\cdot}9$, (- - - - -) and ($m_1/m_b = 0{\cdot}1$).

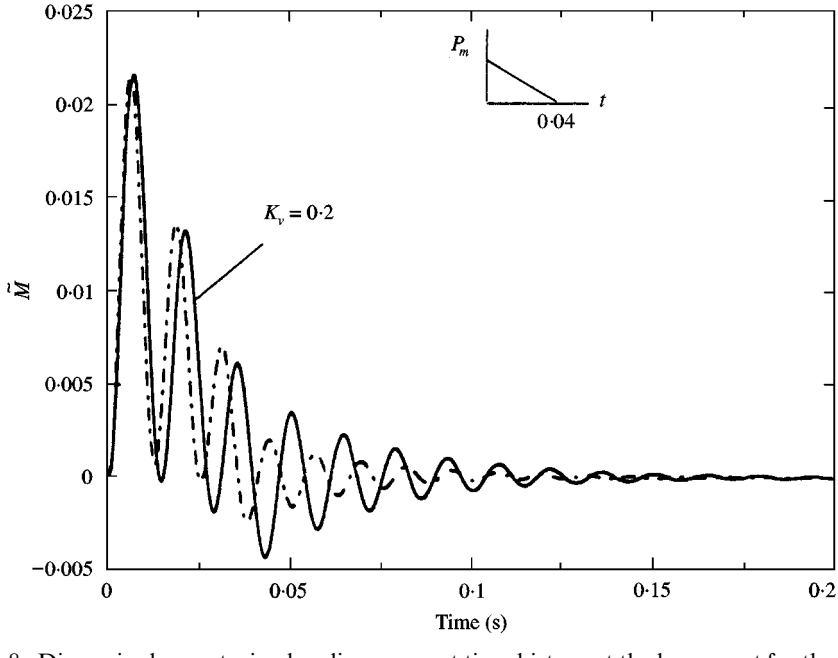

Figure 8. Dimensionless restoring bending moment time-history at the beam root for the activated beam subjected to a triangular blast loading. Two locations of the unistore, $\eta = 0{\cdot}1$ (—·—·), and $\eta = 0{\cdot}9$ (——) are considered. In addition $AR = 8$, $E/G' = 50$, $m_1/m_b = 0{\cdot}1$.

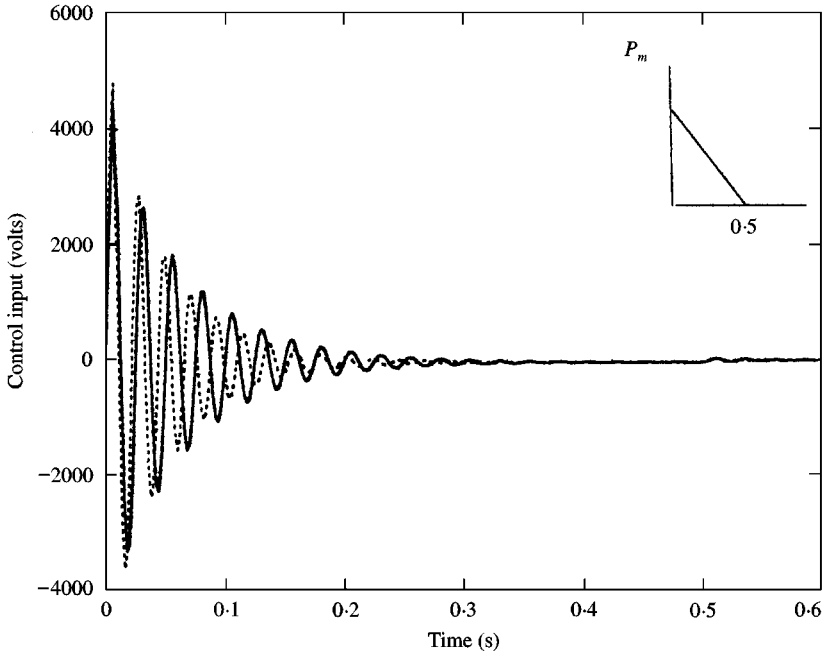

Figure 9. Control input (volts) time history in the case of a blast load. $L = 80$ in; $m_1/m_b = 0{\cdot}1$. The two scenarios for the location of the unistore are: $\eta = 0{\cdot}1$ (- - - - -), and $\eta = 0{\cdot}9$ (——). Transverse shear is discarded.

At the same time, the high efficiency of this control methodology to confine the motion of the structure to such a pressure pulse becomes evident from this figure.

In Figure 8, the closed-loop dimensionless restoring bending moment at the wing-root $\tilde{M} = (\equiv \theta'_x(0)L)$, emerging in the conditions of a blast load is displayed. In this plot two locations of the unistore are considered. The results show that in the free-motion regime, for the store located toward the beam tip, the closed-loop elastic moment is larger than in the case of the store located towards its root.

Finally, in Figure 9 the control input time history in the case of the beam acted on by a triangular blast load and carrying a store is depicted. The results reveal that the control input is rather insensitive to the location of the store.

8. CONCLUSIONS

A methodology based upon adaptive materials technology was applied towards the goal of enhancing the dynamic response of cantilevered beams carrying externally mounted stores, and subjected to time-dependent external loads. The results reveal that the control methodology described here can play a noticeable role of damping the oscillations induced in the structure by the action of time-dependent external excitations.

Moreover, based on the results obtained herewith it can be anticipated that this control methodology is likely to play a significant role toward the aeroelastic control of aircraft wings as well.

REFERENCES

1. O. Song, L. Librescu and C. A. Rogers 1994 *Journal of Intelligent Materials Systems Structures* **5**, 42–48. Adaptive response control of cantilevered thin-walled beams carrying heavy concentrated masses.
2. O. Song, L. Librescu 1996 *International Journal of Mechanical Sciences* **38**, 483–498. Bending vibrations of adaptive cantilevers with external stores.
3. L. Librescu and O. Song 1997 *Structronic Systems*: *Smart Structures*, *Devices and Systems* (H. S. Tzou, editor, Vol **1**, 113–138. Singapore: World Scientific, Static and dynamic behavior of adaptive aircraft wings carrying externally mounted stores.
4. J. Lottati 1987 *Journal of Aircraft* **24**, 793–802. Aeroelastic stability characteristics of a composite swept wing with tip weights for an unrestrained vehicle.
5. H. F. Gern and L. Librescu 1998 *AIAA Journal* **36**, 1121–1129. Static and dynamic aeroelasticity of advanced aircraft wings carrying external stores.
6. H. F. Gern and L. Librescu 1998 *Aerospace Science and Technology* **2**, 321–333. Effect of externally mounted stores on flutter characteristics of advanced swept cantilevered aircraft wings.
7. L. Librescu, L. Meirovitch and O. Song 1996 *Journal of Aircraft* **33**, 203–213. Intergrated structural tailoring and adaptive materials control for advanced aircraft wings.
8. L. Librescu, L. Meirovitch and S. S. Na 1997 *AIAA Journal* **35**, 1309–1315. Control of cantilever vibration via structural tailoring and adaptive materials.
9. A. Gjelsvik 1981 *The Theory of Thin Walled Bars*. New York: Wiley.
10. H. S. Tzou 1993 *Piezoelectric Shells*, *Distributed Sensing and Control of Continua*. Dordrecht: Kluwer Academic Publ.
11. L. Librescu, O. Song and C. A. Rogers 1993 *International Journal of Engineering Science* **31**, 775–792. Adaptive vibrational behavior of cantilevered structures modeled as composite thin-walled beams.
12. L. Librescu, L. Meirovitch and O. Song 1996 *La Recherche Aérospatiale* **1**, 23–25. Refined structural modeling for enhancing vibrations and aeroelastic characteristics of composite aircraft wings.
13. T. Bailey and J. E. Hubbard Jr. 1985 *Journal of Guidance*, *Control and Dynamics* **8**, 605–611. Distributed piezoelectric–polymer active vibration control of a cantilever beam.
14. C. Y. Lin and E. F. Crawley 1995 *Journal of Aircraft* **32**, 1130–1137. Aeroelastic actuation using elastic and induced strain anisotropy.
15. L. Librescu and S. S. Na 1997 *Journal of Acoustical Society of America* **102**, 3516–3522. Vibration and dynamic response control of cantilevers carrying externally mounted stores.
16. A. Baz 1997 *Journal of Vibration and Acoustics*, *ASME* **119**, 166–172. Dynamic boundary control beams using active constrained layer damping.
17. V. Birman and C. W. Bert 1987 *International Journal of Impact Engineering* **6**, 145–155. Behavior of laminated plates subjected to conventional blast.
18. M. J. Crocker 1967 *Journal of the Acoustical Society of America* **42**, 1970. Multimode response of panels to normal and to travelling sonic booms.
19. J. J. Gottlieb and D. V. Ritzel 1988 *Progress in Aerospace Sciences* **25**, 131–188. Analytical study of sonic boom from supersonic projectiles.
20. L. Librescu and A. Nosier 1990 *AIAA Journal* **28**, 345–352. Response of laminated composite flat panels to sonic boom and explosive blast loadings.
21. L. Librescu and A. Nosier 1990 17*th Congress of the International Council of the Aeronautical Sciences*, *Stockholm*, *Sweden*, 2134–2144. *Paper ICAS*-90-1.4*R*. Dynamic response of anisotropic composite panels to time-dependent external excitations.
22. E. F. Crawley 1994 *AIAA Journal* **31** 1689–1699. Intelligent structures for aerospace: a technology and assessment.

23. H. S. Tzou and J. P Zhong 1992 *Active Materials and Adaptive Structures, Materials and Structures Series* (G. J. Knowles, editor). 219–224, Institute of Physics Publ. Adaptive piezoelectric structures: theory and experiment.
24. L. Meirovitch 1997 *Principles and Techniques of Vibrations.* Englewood Cliffs, NJ: Prentice-Hall.
25. D. A. Berlincourt, D. R. Curran and H. Jaffee 1964 *Physical Acoustics—Principles and Methods* (E. P. Mason, editor), Vol. **1**, Part A, 202–204. New York: Academic Press, Piezoelectric and piezomagnetic materials and their function in transducers.